Springer

KSME

Journal of Mechanical Science and Technology 24 (11) (2010) 2215~2220
www.springerlink.com/content/1738-494x
DOI 10.1007/s12206-010-0803-8

Numerical study on spatial distribution of silver nanoparticles inside whole-body type inhalation toxicity chamber †

Jae Ho Cho[1], Atul Kulkarni[2], Hojoong Kim[1], Jin Uk Yoon[3], Jae Hyuck Sung[4], Il Je Yu[5] and Taesung Kim[1,2,*]

[1]*SKKU Advanced Institute of Nanotechnology (SAINT), Sungkyunkwan University, Suwon, 440-746, Korea*
[2]*School of Mechanical Engineering, Sungkyunkwan University, Suwon, 440-746, Korea*
[3]*HCT Co. Ltd., Incheon, Korea*
[4]*Korea Environment & Merchandise Testing Institute, Incheon, Korea*
[5]*Fusion Technology Research Institution, Hoseo University, Asan, Korea*

(Manuscript Received August 24, 2009; Revised April 7, 2010; Accepted July 8, 2010)

Abstract

Silver nanoparticles are among the fastest growing product categories in the nanotechnology industry. Several experimental studies reported earlier for its toxicity and its associated risks. Uniform distribution of nanoparticle concentration in inhalation toxicity exposure chambers is important in the conduct of inhalation experimental evaluation. However, relatively little is known. Several factors, including nanoparticle size, degree of mixing, and chamber design, may influence the nanoparticles distribution in whole-body exposure chamber. In the present work we investigated numerically the silver nanoparticles concentration distribution and particle trajectory in the whole body inhalation toxicity test chamber. A three dimensional numerical simulation was performed using the commercially available computational fluid dynamics code Fluent with two models, discrete phase model (DPM) and fine particle model (FPM) to calculate spatial particle trajectories and concentration. The simulated results show that the silver nanoparticle trajectories and concentration distribution are dependent on inhalation toxicity chamber geometry.

Keywords: Silver nanoparticles; Numerical study; CFD; Inhalation toxicity

1. Introduction

Silver nanoparticles are emerging as one of the fastest growing nano-materials with wide range of applications. Currently, little is known about the adverse effects of silver nanoparticles to human health and their fate in ecological systems [1-3]. In the mean time, with the recent advances in nanotechnology, silver nanoparticles are being utilized in an increasing number of fields, such as antibacterial materials, antistatic materials, cryogenic superconducting materials, and biosensor materials [4, 5].

Yet, this increasing use of silver nanoparticles necessitates a health and environmental risk assessment of nanoparticles [4, 6]. Exposure to these materials during manufacturing and use can occur through inhalation, dermal contact, and ingestion.

To simulate particle behavior in fluids, two models coupled with computational fluid dynamics (CFD), which are discrete phase model (DPM) and fine particle model (FPM), have been utilized by numerous groups to examine particle deposition in the respiratory tract of humans and animals [7-10].The FPM has gained its popularity on studying particle concentration distributions in indoor environments [11-13], whereas DPM is mainly used to predict the overall particle dispersion pattern [14]. To the best of our knowledge, the behavior of the silver nanoparticles in the inhalation toxicology test chamber was not well studied especially for spatial particle concentration and particle trajectories.

Hence in this work, a three dimensional numerical simulation was performed using the commercially available computational fluid dynamics code Fluent and its plugin models to study the spatial distribution of silver nanoparticles inside the whole body type inhalation toxicity chamber arranged in order. References should be cited in the main text by numerals in a square bracket [1-3].

2. Modeling

2.1 Material and method

The inhalation toxicity test chamber is a chamber system to expose the test animal under test for certain durations and

† This paper was recommended for publication in revised form by Associate Editor Gihun Son

*Corresponding author. Tel.: +82 31 290 7466, Fax: +82 31 290 5889
E-mail address: tkim@skku.edu

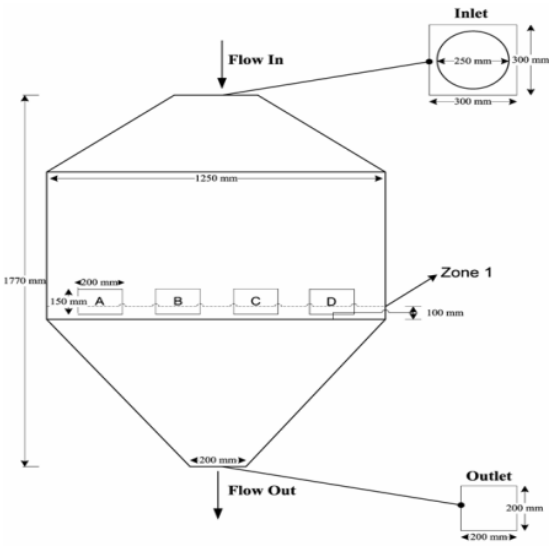

Fig. 1. Schematic of the inhalation toxicity chamber used for simulation study where A, B, C and D are the l cages location.

doses with the aid of nanoparticles. A schematic of the whole body type inhalation toxicity chamber, hence forth referred to as exposure chamber in the text, used for evaluation is depicted in Fig. 1.

The exposure chamber dimensions and test conditions are as described earlier [15]. The inside dimensions of the hexagonal exposure chamber are 0.95 m, 1.25 and 1.77 m (length, width and height, respectively). The inlet nozzle diameter is 0.25 m, where as the outlet nozzle shape is square having length of 0.20m. The air flow rate is considered to be 200 lpm, is similar to the experimental conditions to achieve 10 air changes per hour in the exposure chamber. The location of the animal cage, without animals, under test is denoted as zone 1 in Fig. 1, and is the area of our interest to estimate the silver nanoparticle concentration and flow field trajectory.

The time-averaged Navier-stokes equations describe the motion of the turbulent airflow which is treated as 3-D steady incompressible and isothermal in the exposure chamber. Near the inlet and outlet the calculated Reynolds number is above 2500, hence the turbulent flow was solved using the standard k-ε model and the SIMPLE algorithm is applied to compute the pressure corrections during iteration procedure. The convection terms are discretized using the upwind scheme which is the first order in space. The concept of residuals was used in order to ascertain that the iteration process had converged less than 10^{-5} to a stable solution. The required total simulation time is approximately 100 hours on a Pentium 4 computer with 4 GB ram.

For the particle trajectory, the Lagrangian method is simulated with discrete phase model (DPM) and the Eulerian method is simulated with fine particle model (FPM) for particle concentration. In order to reduce the calculation time and to get optimal results, a 5mm mesh was constructed and optimized using GAMBIT software as depicted in Fig. 2.

Table 1. Silver nanoparticles properties considered during simulations.

Silver NP Conc.	GMD	GSD	Total number conc.#/m^3	Surface area Nm^2/m^3
High	18.93	1.59	2.85×10^{12}	6.61×10^{15}
Middle	18.33	1.12	1.43×10^{12}	2.37×10^{15}
Low	18.12	1.42	6.64×10^{11}	1.08×10^{15}

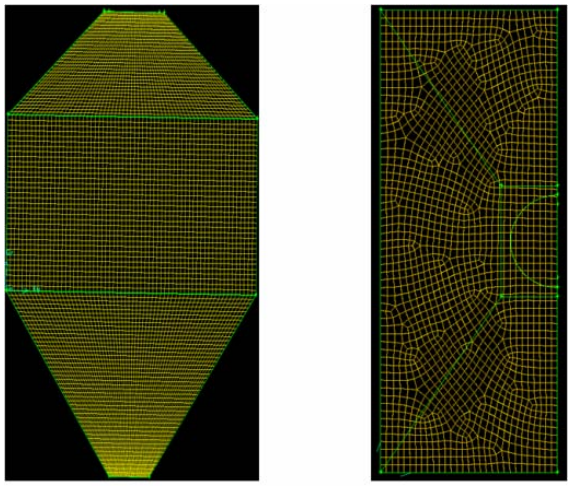

(1) (2)

Fig. 2. Grid shape formed using GAMBIT of the inhalation toxicity chamber at 1)"X" axis and 2) "Z" axis.

The uniform hexagonal shape grid distribution is used for only the Z direction of the exposure chamber. During simulation we considered three types of silver nanoparticle concentrations.

The silver nanoparticles physical properties considered during this simulation studies are same as reported earlier in the experimental study by Sung et.al. [15]. In case of DPM we considered mono-sized particles (305 numbers of silver nanoparticles having 20 nm diameters) as it is very difficult to track many particles simultaneously and may take longer computation time. For FPM we injected particles having size distribution (poly-dispersed), the detail of silver nanoparticles geometric mean diameter (GMD), geometric standard deviation (GSD), total number concentration, and surface area are depicted in Table 1.

It is observed that the silver nanoparticles differ in size distribution; we are not correlating nanoparticle size distribution to simulation results for the change in particle concentration in the whole body exposure chamber.

2.2 Discrete phase model

To predict the trajectory of discrete phase silver nanoparticles, integration of the force balance on the particle written in a Lagrangian reference frame in Fluent DPM has been used. This force balance presents as equation between the particle in-ertia and the forces acting on the particle, is as given in Eq.

(1),

$$\frac{d\overrightarrow{u_p}}{dt} = \overrightarrow{F_D}\left(\vec{u} - \overrightarrow{u_p}\right) + \frac{\vec{g}\left(\rho_p - \rho\right)}{\rho_p} + \overrightarrow{F_E} \tag{1}$$

The left hand side of Eq. (1) represents the inertial force per unit mass (ms^{-2}), where $\vec{u}_p$ is the particle velocity vector. The first term on the right hand side of Eq. (1) is the drag term, where $\overline{F}_D$ the inverse of relaxation time (s^{-1}) and $\vec{u}$ is the air velocity. As particle size is in the nanometer range, the particle Reynolds number is much smaller than one. Hence we considered the drag force per unit mass $\overline{F}_D$ in the Stokes' regime which is stated as Stokes' Law and is defined as given in Eq. (2).

$$F_D = \frac{18\mu}{\rho_p d_p^2 C_c} \tag{2}$$

where μ is viscosity of the air; ρ_p is the particle density; d_p is particle diameter and C_c is the Cunningham correction to Stokes' drag law. Stokes' law assumes that relative velocity of the air at the particle surface is zero, but as the particle size is in nanometer range air molecules were get "slip" at the surface of the particle, hence the resulted particle velocity is much faster than the predicted using Stokes' law. So we considered the slip correction factor Cc as given in Eq. (3).

$$C_C = 1 + \frac{2\lambda}{d_p}\left(1.257 + 0.4e^{-(1.1d_p/2\lambda)}\right) \tag{3}$$

where λ is the molecular mean free path.

The second term of Eq. (1) is for the gravity and the buoyancy, where ρ and ρ_p are the density of the air and the particles, respectively. As described earlier the particles used are in the range of nanometer, we considered the Brownian motion for the particle trajectory where it can be considered as Brownian force which is a random force as stated in Eq. (4).

$$F_E = \varsigma_i \sqrt{\frac{\pi S_0}{\Delta t}} \tag{4}$$

where ς_i are zero-mean, unit variance-independent Gaussian random numbers, ∇ t is time step of particle trajectory. S_0 is proportional to the minus fifth power of particle size which means that when the particle size is reduced, the value of S_0 increases dramatically.

2.3 Fine particle model

The Eulerian method along with general dynamic equation (GDE) is used here for particle concentration estimation as defined in Eq. (5).

$$\frac{\partial M_0}{\partial t} = conv + ext + diff + coag \tag{5}$$

By applying the standard definitions of the GDE, we can evaluate various phenomena related to particle size distribution moments M_0 considering the effect of convective transport ($conv$), transport by external forces (ext) , diffusion ($diff$) and coagulation ($coag$) in the inhalation chamber. The moment distribution M_0 means 0^{th} moment of particle size distribution which is implies the particle number concentration distribution. Thus in this study, the final result from FPM is the number concentration change of particle size distribution.

Due to the air velocity distribution inside the inhalation chamber which affects the particle number concentration at the given location by convective motion can be given by Eq. (6).

$$conv = -\nabla \cdot \left[\overline{u} M_0\right] \tag{6}$$

External forces are created by processes like thermophoresis, gravitational settling (sedimentation), and electrical and magnetic forces. In our case, the external force is mainly due to gravitational settling. Under these conditions, the external force can be used to calculate an additional particle velocity as given in Eq. (7).

$$ext = -\nabla \cdot \left[\overline{u}_{ext} M_0\right] \tag{7}$$

Here, $\overline{u}_{ext}$ is the terminal settling velocity of the particle. This term came from the force balance between gravitational force and drag force in the Stokes regime and is given as Eq. (8).

$$u_{ext} = \frac{\rho_{p,} C_c g d_p^2}{18\mu} \tag{8}$$

The diffusion term in the FPM is represented as given in Eq. (9). As stated earlier the particles are in the nanometer range, the diffusion coefficient is much higher than for that bigger particles hence we considered the concentration change caused by Brownian motion.

$$diff = \nabla \cdot \left[\rho_g \overline{D} \nabla \frac{M_0}{\rho_g}\right] \tag{9}$$

The "Moment diffusivity" $\overline{D}$ is given by Eq. (10), is nothing but averaged diffusion coefficient for the particle size distribution.

$$\overline{D} = M_0^{-1} \int_0^{\infty} D_p\left(d_p\right) n\left(d_p\right) dp_p \tag{10}$$

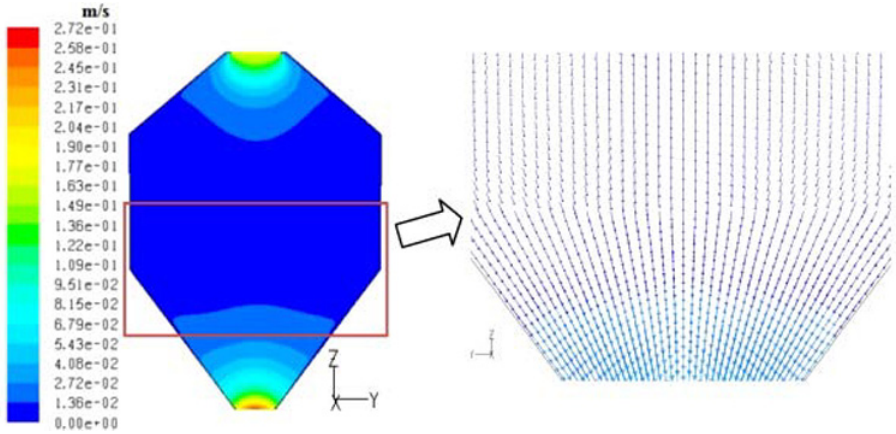

Fig. 3. Air velocity contour simulated by FPM at "X" axis for silver nanoparticle concentration along with velocity vectors.

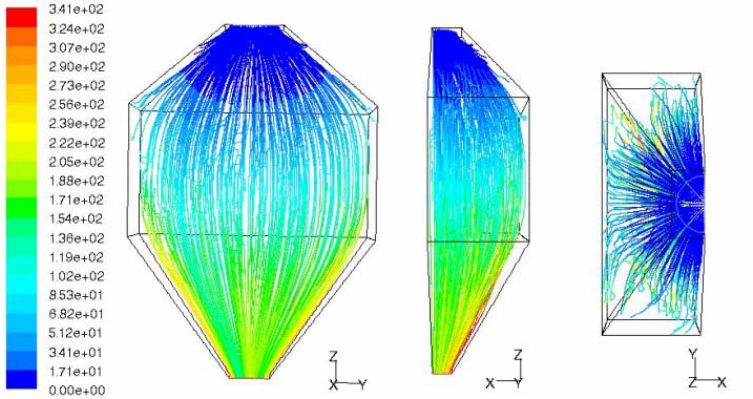

Fig. 4. Silver nanoparticles trajectories in the inhalation toxicity chamber simulated by DPM for 5 mm mesh size at 1) "X" axis, 2) "Y" axis and 3) "Z" axis.

and the particle diffusion coefficient can be expressed as:

$$D_p\left(d_p\right)=\frac{k_B T}{3\pi\mu d_p}C_c \tag{11}$$

where k_B is the Boltzmann constant and T is surrounding air temperature and which is ambient temperature. The FPM represents Brownian diffusion according to the diffusion coefficient defined in Eq. (11) with the integrand function Brownian diffusion.

Coagulation is the only physical process by which the equations for the moments of different modes are directly coupled. When two particles collide, they are removed from the modes to which they belonged, and the resulting new particle is added to a mode. The coagulation terms are divided into "gain" and "loss" terms. As the nanoparticles are mono dispersed and we considered the 0^{th} moment only which implies that the number concentration decreases when coagulation happens nothing but loss.

3. Results and discussion

The air velocity contour was calculated with 5mm mesh using Eulerian method and the observed results were depicted in Fig. 3. We observed that, the air velocity is decreased from about 0.15 m/s to almost 0 m/s at the middle of the exposure chamber and again increase in air velocity up to about 0.27 m/s at the outlet of the exposure chamber. This phenomenon is mainly due to the exposure chamber shape. This implies that the silver nanoparticle dispersion in middle of the exposure chamber will not be affected by the convective motion of the air flow. Initially we assumed that there might be turbulence near the inlet and outlet of the exposure chamber. The flow velocity vectors shown in Fig. 3 indicate that there is minute turbulence near the inlet and outlet of the chamber. However, there is no turbulence in the middle of the exposure chamber and around zone 1.

The results of the silver nanoparticle trajectories and residence time from DPM along x, y and z plane is shown in Fig. 4.

Particle transport simulation results reveal that nearly 80% of the silver nanoparticles escaped from the outlet of the exposure chamber and 20% were either deposited on the chamber wall or suspended in the chamber. We assumed that these remaining 20% silver nanoparticles has negligible effect on change in total number concentration hence we ignored its

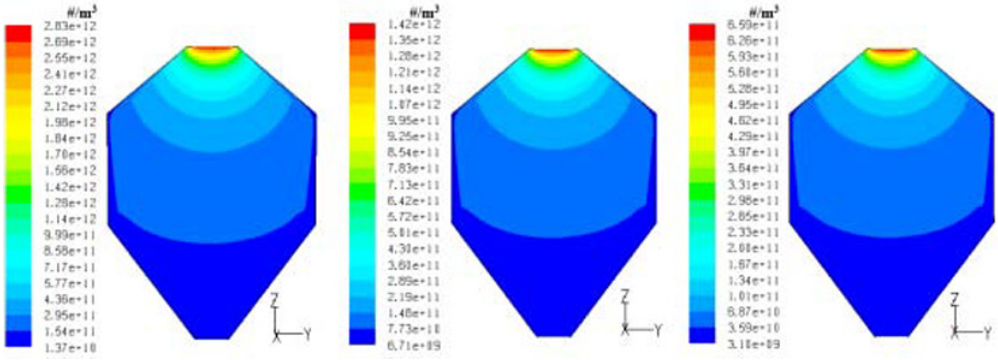

(a) (b) (c)

Fig. 5. Silver nanoparticle concentration in the inhalation toxicity chamber simulated by FPM at "X" axis for a) high, b) middle and 3) low silver nanoparticle concentrations.

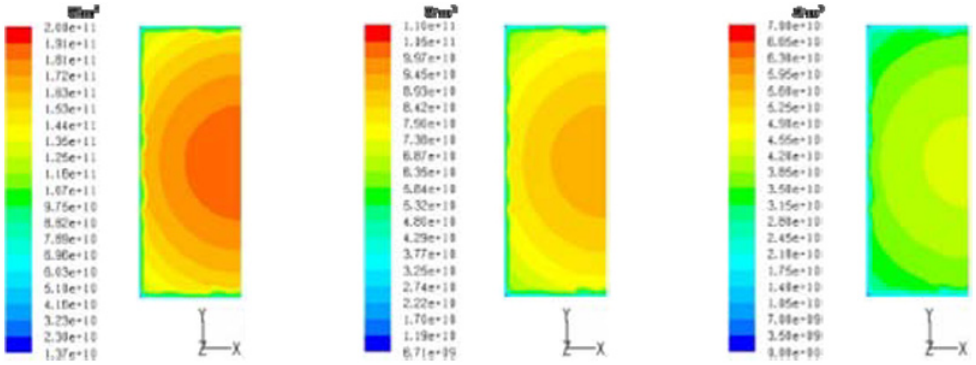

(1) (2) (3)

Fig. 6. Silver nanoparticle concentration in the inhalation toxicity chamber simulated by FPM at Zone 1 for 1) high, 2) middle and 3) low silver nanoparticle concentrations.

effect during simulation.

Since the air flow is laminar in the middle of the exposure chamber, even distribution of silver nanoparticles can be achieved despite the Brownian diffusion, although there can be a loss of silver nanoparticles near the wall. The particle motion is linear in the Z axis because these particles follow the air stream line; hence we observed that the Brownian force has little effect on the particle trajectories. The particle residence time is also estimated by DPM and which is the time is taken by the silver nanoparticle to travel from the inlet to the outlet of the exposure chamber. The average residence time of silver nanoparticles was found to be approximately 230 seconds. This also indicates that there is negligible coagulation of silver nanoparticles in the exposure chamber, since coagulation rate depends on the square of concentration, and thus dominates behavior at high concentrations but is negligible at low concentrations. Simple estimates of variations in aerosol number concentration resulting from coagulation (assuming no growth following collisions) show that a 50% reduction in concentration is expected within 20 s at concentrations of 1014 particles/m^3, and within 55 h at concentrations of 1010 particles/m^3 [16], however in our case the estimated residence time is too short. Hence, as the coagulation effect is not significant the results from DPM are restricted to get single particle trajectory only.

The vertical distribution of the silver nanoparticle concentration in the exposure chamber was systematically studied for the three particle concentrations as depicted in Fig. 5.

To get the feel of the effect of particle concentration, the range legends are adjusted accordingly. For all three particle concentrations, the even spread of silver nanoparticles are up to the middle section of the chamber in vertical plane due to increase in the volume of the chamber and decrease in the air flow rate.

Near the inlet the particle concentration is high as compared with outlet of the exposure chamber; however, there is uniform particle distribution around zone 1 of the whole body exposure chamber.

We evaluated the horizontal distribution of silver nanoparticle concentrations, as depicted in Fig. 6. The simulated results are at zone 1 from the bottom plane of the middle of the exposure chamber. We evaluated zone 1 because, this is the breathing zone of the animal under test. From the results we can see that at the location B and C the silver nanoparticle concentration is almost same, however, the location A and D has up to 15% of silver nanoparticle concentration variation.

These observations were obtained in the exposure chamber without animals. This little variation is anticipated by the ex-

perimentalist; hence the test animal cages in the whole body exposure chamber were relocated time to time.

4. Conclusions

In this paper, spatial distribution of the silver nanoparticles inside whole body inhalation toxicity chamber is studied numerically by computational fluid dynamics (CFD). As revealed by simulation the particle trajectories are dependent on the inhalation toxicity chamber geometry. The particle concentration depends principally on two parameters, the chamber shape and the particle deposition on the side wall of the chamber. Around zone 1, the silver nanoparticle concentration is almost uniform and has low particle velocity which enables the animal under test to inhale the maximum number of particles.

Acknowledgment

The authors would like to acknowledge the KEMTI and HCT in Korea where this work was performed and this project is funded by the Korea Research Foundation.

References

[1] L. Molhave, S. K. Kjaergaard and J. Attermann, Sensory and other neurogenic effects of exposures to airborne office dust. *Atmos. Environ.* 34 (2000) 4755-4766.

[2] M. J. Mendell, W. J. Fisk, M. R. Petersen, C. J. Hines, M. Dong, D. Faulkner, J. A. Deddens, M. Ruder, D. Sullivan and M. F. Boeniger, Indoor particles and symptoms among office workers: Results from a double-blind cross-over study. *Epidemiology* 13 (2002) 296-304.

[3] T. Schneider, J. Sundell, W. Bischof, M. Bohgard, J. W. Cherrie, P. A. Clausen, S. Dreborg, J. Kildeso, S. K. Kjaergaard, M. Lovik, P. Pasanen and K. Skyberg, 'EUROPART'. Airborne particles in the indoor environment. A European interdisciplinary review of scientific evidence on associations between exposure to particles in buildings and health effects. *Indoor Air* 13 (2003) 38-48.

[4] Z. Zhang and Q. Chen, Experimental measurements and numerical simulations of particle transport and distribution in ventilated rooms. *Atmos. Environ* 40 (2006) 3396-3408.

[5] S. A. Blaser, M. Scheringer, M. MacLeod and K. Hungerbuhler, Estimation of cumulative aquatic exposure and risk due to silver: Contribution of nano-functionalized plastics and textiles. *Sci. Total Environ* 390 (2008) 396-409.

[6] K. L. Dreher, Health and environmental impact of nanotechnology: Toxicological assessment of manufactured nanoparticles. *Toxicol. Sci* 77 (2004) 3-5.

[7] A. Riddle, D. Carruthers, A. Sharpe, C. McHugh and J. Stocker, Comparisons between FLUENT and ADMS for atmospheric dispersion modeling. *Atmos. Environ* 38 (2004) 1029-1038.

[8] Z. Zhang and Q. Chen, Comparison of the Eulerian and Lagrangian methods for predicting particle transport in enclosed spaces. *Atmos. Environ* 41 (2007) 5236-5248.

[9] K. R. Minard, D. R. Einstein, R. E. Jacob, S. Kabilan, A. P. Kuprat, C. A. Timchalk, L. L. Trease and R. A. Corley, Application of Magnetic Resonance (MR) Imaging for the Development and Validation of Computational Fluid Dynamic (CFD) Models of the Rat Respiratory System. *Inhal. Toxicol* 18 (2006) 787-794.

[10] M. J. Oldham, Challenges in Validating CFD-Derived Inhaled Aerosol Deposition Predictions. *Inhal. Toxicol* 18 (2006) 781-786.

[11] S. Murakami, S. Kato, S. Nagano and S. Tanaka, Diffusion characteristics of airborne particles with gravitational settling in a convection-dominant indoor flow field. *ASHRAE Transactions* 110 (1992) 88-95.

[12] B. Zhao, Z. Zhang, X. Li and D. Huang, Comparison of diffusion characteristics of aerosol particles in different ventilated rooms by numerical method. *ASHRAE Transactions* 110 (2004) 88-95.

[13] B. Zhao, Z. Zhang and X. Li, Numerical study of the transport of droplets or particles generated by respiratory system indoors. *Building and Environment* 40 (2005) 1032-1039.

[14] C. Beghein, Y. Jiang and Q. Y. Chen, Using large eddy simulation to study particle motions in a room. *Indoor Air* 15 (2005) 281-290.

[15] J. H. Sung, J. H. Ji, J. U. Yoon, D. S. Kim, M. Y. Song, J. Jeong, B. S. Han, J. H. Han, Y. H. Chung, J. Kim, T. S. Kim, H. K. Chang, E. J. Lee, J. H. Lee and I. J. Yu, Lung function changes in Sprague-Dawley rats after prolonged inhalation exposure to silver nanoparticles. *Inhal. Toxicol* 20 (2008) 567-574.

[16] W. C. Hind, Aerosol Technology: properties, behavior, and measurement of airborne particles, John Wiley and Son, Inc., New York, 1999.

Jaeho Cho received the Master's degree in 2009 from the SKKU Advanced Institute of Nanotechnology, Sungkyunkwan University, Korea. He is currently worked for HCT Inc. in South Korea. His research interest is inhalation toxicity chamber and heating, ventilation and air-conditioning (HAVC) of indoor air.

Taesung Kim received the Ph.D. degree in 2003 from the Department of Mechanical Engineering, University of Minnesota, Twin Cities Campus, USA. He is currently a Professor in the School of Mechanical Engineering, Sungkyunkwan University, South Korea. His research interests are in nanoparticle instrumentation and manufacturing, nano/micro contamination and atmospheric aerosol control, nanogrinding/CMP, nanostructured material research, and sensors.